Similarities and differences when solving Helmholtz problems with Schwarz Domain Decomposition and Multigrid

Martin J. Gander[0000−0001−8450−9223] and Yafei Sun[0009−0008−7512−9550]

1 Introduction

As a fundamental model for time-harmonic wave propagation, the Helmholtz equation captures the essential numerical challenges inherent in wave propagation computations. Despite its apparent simplicity, it embodies many of the key difficulties encountered in solving high-frequency wave problems. Due to the wide range of scientific and engineering applications involving time-harmonic waves, the numerical solution of the Helmholtz equation has been extensively studied, see [5, 9, 12] and the review [10] for domain decomposition methods , and [1, 6, 7, 8, 13] for multigrid techniques. Recently, an analysis for the 2D Helmholtz equation on a bounded domain revealed that the convergence factor of the Schwarz methods is strongly influenced by the outer boundary conditions (BCs) [11]: convergence for free space problems is much better than for cavity problems. As an iterative method of equal importance to domain decomposition, a natural question is whether the convergence behavior of multigrid methods is also strongly dependent on the physical outer BCs, and whether free space problems are also much easier to solve with multigrid than cavity problems. This is the motivation for our present study.

We use as our model problem the 1D Helmholtz equation

$$\begin{aligned} (\Delta + k^2)u &= f \ \text{ in } \Omega = (0,1),\\ \partial_x u - pu &= 0 \ \text{ at } x = 0,\\ \partial_x u + pu &= 0 \ \text{ at } x = 1, \end{aligned} \tag{1}$$

where $k > 0$ is the wave number, and $f \in L^2(\Omega)$ is the source term. When the parameters $p = ik, i = \sqrt{-1}$, we obtain impedance BCs and the problem corresponds

Martin J. Gander
University of Geneva, Department of Mathematics, e-mail: martin.gander@unige.ch

Yafei Sun
Jilin University, School of Mathematics, e-mail: yafei.sun@unige.ch

to a free space problem, while $p \to \infty$ leads to Dirichlet BCs and the problem is a cavity problem. We will compare the convergence behavior of domain decomposition and multigrid for these two situations.

Note that the simple 1D setting here allows for the explicit derivation of convergence factors for the Schwarz method, as well as for the formulation of the basic two-grid operator for multigrid methods. This enables straightforward parameter optimization and facilitates a systematic numerical investigation of their convergence behavior. As will be shown numerically in the subsequent sections, multigrid methods exhibit markedly different behavior from Schwarz methods in the 1D Helmholtz setting: convergence is equally poor for both free space and cavity problems. Even though for domain decomposition the 1D setting is a bit oversimplified, because the absorbing boundary conditions become local, simple impedance conditions, the results we obtain are also relevant for Schwarz methods in higher dimensions, as it was observed using semi-analytical Fourier analysis in [11]. This observation motivates the expectation that similar convergence differences may persist for multigrid methods applied to higher-dimensional Helmholtz problems. Moreover, while only pure Dirichlet and Robin BCs are considered in this work, the effects of mixed BCs can also be investigated similarly, where the interplay between absorbing and reflecting boundaries may further influence convergence properties. A rigorous analysis of such cases is beyond the scope of the present paper and is left for future work.

2 Schwarz Domain Decomposition Methods for Helmholtz

We now introduce Schwarz domain decomposition methods for solving the 1D Helmholtz problem (1). We only consider the case of two-subdomains, the case of multiple subdomains could be done following the techniques in [4]: we divide the computational domain $\Omega = (0, 1)$ into two overlapping subdomains $\Omega_1 := (0, \beta)$ and $\Omega_2 := (\alpha, 1)$ with overlap $L := \beta - \alpha > 0$. Then the optimized parallel Schwarz method starts from an initial guess $\{u_1^0, u_2^0\}$ and computes for $\ell \geq 1$ until convergence

$$\begin{array}{llll} (\Delta+k^2)u_1^\ell = f & \text{in } \Omega_1, & (\Delta+k^2)u_2^\ell = f & \text{in } \Omega_2, \\ \partial_x u_1^\ell - p u_1^\ell = 0 & \text{at } x=0, & \partial_x u_2^\ell + p u_2^\ell = 0 & \text{at } x=1, \\ \partial_x u_1^\ell + p_1 u_1^\ell = \partial_x u_2^{\ell-1} + p_1 u_2^{\ell-1} & \text{at } x=\beta, & \partial_x u_2^\ell - p_2 u_2^\ell = \partial_x u_1^{\ell-1} - p_2 u_1^{\ell-1} & \text{at } x=\alpha, \end{array} \qquad (2)$$

where Robin transmission conditions $\partial_x + p_1$ and $\partial_x - p_2$ are imposed at the interfaces $x = \beta$ and $x = \alpha$. Here $p_1, p_2 \in \mathbb{C}$ are transmission parameters, which are important for the performance of the method. The selection of them is generally guided by an analysis of the associated iteration operator, typically through the study of its spectral properties or convergence factors, with the aim of achieving best convergence of the algorithm. As discussed in the following sections, optimal or near-optimal parameter values can be identified directly from the explicit expression of the convergence factors in simplified settings (e.g., the 1D case), or determined via optimization techniques in more general situations (e.g., higher-dimensional cases)[9, 10, 11, 4]. When the parameters p_1 and p_2 tend to infinity, we obtain the classical parallel Schwarz method.

To analyze the convergence behavior of the parallel Schwarz method (2), we introduce the error $\hat{e}_j^\ell := u - u_j^\ell, j = 1, 2$, which by linearity satisfies the same algorithm (2), but with zero data. Solving the ordinary differential equations in the corresponding error iteration, we obtain using the outer Robin BCs for each wave number k the solutions

$$\hat{e}_1^\ell(x) = A_1^\ell(k)\left(e^{ikx} + \frac{ik-p}{ik+p}e^{-ikx}\right),\ \hat{e}_2^\ell(x) = B_2^\ell(k)\left(e^{-ikx} + \frac{ik-p}{ik+p}e^{-ik(2-x)}\right).$$

To determine the two remaining constants $A_1^\ell(k)$ and $B_2^\ell(k)$ we insert the solutions into the Robin transmission conditions in (2), which leads to

$$\begin{aligned} A_1^\ell &= \frac{(p_1-ik)e^{-ik\beta}+(p_1+ik)\frac{ik-p}{ik+p}e^{-ik(2-\beta)}}{(p_1+ik)e^{ik\beta}+(p_1-ik)\frac{ik-p}{ik+p}e^{-ik\beta}}B_2^{\ell-1} =: \rho_1(k,p,p_1)B_2^{\ell-1},\\ B_2^\ell &= \frac{(p_2-ik)e^{ik\alpha}+(p_2+ik)\frac{ik-p}{ik+p}e^{-ik\alpha}}{(p_2+ik)e^{-ik\alpha}+(p_2-ik)\frac{ik-p}{ik+p}e^{-ik(2-\alpha)}}A_1^{\ell-1} =: \rho_2(k,p,p_2)A_1^{\ell-1}. \end{aligned} \tag{3}$$

Let $\alpha^\pm := [\beta \pm (2-\beta)]/2$, $\beta^\pm := [\alpha \pm (2-\alpha)]/2$. From (3) we then get the convergence factor $\rho := \rho_1\rho_2$ of the parallel Schwarz method (2) to be

$$\rho = \frac{(-pp_1-k^2)\sin(k\alpha^-)+(p_1k-pk)\cos(k\alpha^-)}{(pp_1-k^2)\sin(k\beta)+(p_1k+pk)\cos(k\beta)}\,\frac{(pp_2+k^2)\sin(k\alpha)+(p_2k-pk)\cos(k\alpha)}{(-pp_2+k^2)\sin(k\beta^-)+(p_2k+pk)\cos(k\beta^-)}. \tag{4}$$

Adjusting the values of the parameters (p, p_1, p_2), we can obtain the convergence factors we are interested in (overlap $L := \beta - \alpha$ in what follows):

$$\rho_{\text{Cla}}^{\text{Cavity}} = \frac{\sin(k(\beta-1))\sin(k\alpha)}{\sin(k\beta)\sin(k(\alpha-1))}, \qquad (p = p_1 = p_2 \to \infty) \tag{5}$$

$$\rho_{\text{Opt}}^{\text{Cavity}} = \frac{(p_1\sin k(\beta-1)+k\cos k(\beta-1))(p_2\sin k\alpha-k\cos k\alpha)}{(p_1\sin k\beta+k\cos k\beta)(p_2\sin k(\alpha-1)-k\cos k(\alpha-1))}, \qquad (p\to\infty) \tag{6}$$

$$\rho_{\text{Cla}}^{\text{Free}} = e^{-ik2L}, \qquad (p = ik,\ p_1 = p_2 \to \infty) \tag{7}$$

$$\rho_{\text{Opt}}^{\text{Free}} = \frac{p_1-ik}{p_1+ik}\cdot\frac{p_2-ik}{p_2+ik}\cdot e^{-ik2L}. \qquad (p = ik) \tag{8}$$

We see already that the classical Schwarz method for the free space problem does not converge, since the contraction factor $|\rho_{\text{Cla}}^{\text{Free}}| = 1$ in (7). A numerical investigation of their convergence behavior, together with that of multigrid, will be presented in the subsequent sections.

3 Multigrid Methods for Helmholtz

Now for the multigrid method, we focus only on the two-grid case, as it serves as a fundamental component of the multigrid hierarchy. By discretizing problem (1) using a standard centered finite-difference scheme on a uniform mesh $\Omega^h := \{x_j = jh : j = 0, 1, \ldots, N+1\}, h = \frac{1}{N+1}$, we obtain a linear system of the form

$A\mathbf{u} = \mathbf{f}$ for approximating the solution $u_j \approx u(x_j)$. For the Dirichlet BC ($p \to \infty$), we have $\mathbf{u} = [u_1, u_2, \dots, u_N]$, $A = \frac{1}{h^2}\text{tridiag}\left(-1, 2-k^2h^2, -1\right)$ and $\mathbf{f} = \left(f(x_j)\right)_{j=1}^{N}$. For the Robin BC ($p = ik$), we need to include the boundary unknowns, $\mathbf{u} = [u_0, u_1, \dots, u_{N+1}]$, $\mathbf{f} = \left(f(x_j)\right)_{j=0}^{N+1}$, and

$$A = \frac{1}{h^2}\begin{bmatrix} 2-k^2h^2-i2kh & -2 & & & \\ -1 & 2-k^2h^2 & -1 & & \\ & \ddots & \ddots & \ddots & \\ & & -1 & 2-k^2h^2 & -1 \\ & & & -2 & 2-k^2h^2-i2kh \end{bmatrix}, \tag{9}$$

where we approximated the Robin BCs by second-order centered finite differences,

$$\frac{u_{-1}-u_1}{2h} - iku_0 = 0, \quad \frac{u_{N+2}-u_N}{2h} - iku_{N+1} = 0.$$

We introduce the coarse grid $\Omega^H := \left\{x_j = jH : j = 0, 1, \dots, n+1\right\}$ with $n = \frac{N-1}{2}$, $H = 2h$, and let A_H be the discrete Helmholtz operator on Ω^H like for A. Then, the two-grid method for the linear system $A\mathbf{u} = \mathbf{f}$ is given by performing for $m = 0, 1, \dots$ [1, 7, 3]

$$\begin{cases} \tilde{\mathbf{u}}^m := S^{\nu_1}(\mathbf{u}^m, \mathbf{f}); & \text{\% pre-smoothing} \\ \mathbf{r} := R(\mathbf{f} - A\tilde{\mathbf{u}}^m); & \text{\% restrict residual} \\ \mathbf{e} = A_H^{-1}\mathbf{r}; & \text{\% coarse-grid correction} \\ \tilde{\mathbf{u}}^{m+1} = \tilde{\mathbf{u}}^m + P\mathbf{e}; & \text{\% add coarse correction} \\ \mathbf{u}^{m+1} = S^{\nu_2}(\tilde{\mathbf{u}}^{m+1}, \mathbf{f}); & \text{\% post-smoothing} \end{cases} \tag{10}$$

where $\mathbf{u}^0$ is an initial guess, S^ν denotes ν iterations of a smoother S, P is a prolongation operator, and R is a restriction operator, which will be defined more precisely below. The two-grid algorithm (10) is a stationary iterative method, and its iteration matrix (also called the *two-grid operator*) is given by [1]

$$T = S^{\nu_2}CS^{\nu_1} = S^{\nu_2}\left(I - PA_H^{-1}RA\right)S^{\nu_1}. \tag{11}$$

To achieve a fast-converging two-grid algorithm (10), an efficient smoother and coarse grid correction are required. Inspired by the techniques proposed in [7], we consider using a multi-step damped Jacobi smoother consisting of multiple consecutive smoothing steps, each with its own damping parameter $\omega_i, i = 1, \dots, s$,

$$\begin{cases} \bar{\bar{\mathbf{u}}}^1 = \mathbf{u}^m + \omega_s D^{-1}(\mathbf{f} - A\mathbf{u}^m) = (I - \omega_s D^{-1}A)\mathbf{u}^m + \omega_s D^{-1}\mathbf{f}, \\ \bar{\bar{\mathbf{u}}}^2 = \bar{\bar{\mathbf{u}}}^1 + \omega_{s-1}D^{-1}(\mathbf{f} - A\bar{\bar{\mathbf{u}}}^1) = (I - \omega_{s-1}D^{-1}A)\bar{\bar{\mathbf{u}}}^1 + \omega_{s-1}D^{-1}\mathbf{f}, \\ \vdots \\ \mathbf{u}^{m+1} = \bar{\bar{\mathbf{u}}}^{s-1} + \omega_1 D^{-1}(\mathbf{f} - A\bar{\bar{\mathbf{u}}}^{s-1}) = (I - \omega_1 D^{-1}A)\bar{\bar{\mathbf{u}}}^{s-1} + \omega_1 D^{-1}\mathbf{f}, \end{cases} \tag{12}$$

where $D := \mathrm{diag}(A)$ and $\mathbf{u}^m$ is the calculated solution at iteration m. The corresponding iteration matrix is

$$S_{\omega_1,\ldots,\omega_s} := (I - \omega_1 D^{-1}A)(I - \omega_2 D^{-1}A)\cdots(I - \omega_s D^{-1}A). \tag{13}$$

Note that when $s = 1$, we obtain the classical damped Jacobi iteration, and $s = 2$ leads to the two-step damped Jacobi iteration studied in [7].

For the coarse grid correction $C = I - PA_H^{-1}RA$, we use the standard linear interpolation operator P, and full weighting restriction for R. Their matrix representations are provided in [7, Eq. (3.1), Eq. (3.4)], from which it follows that P and R satisfy $R = \frac{1}{2}P^\top$. Such a standard coarse-grid correction is however insufficient to produce an efficient two-grid algorithm for the Helmholtz equation: as shown in [7, Section 3.2] for the case of Dirichlet boundary conditions, the eigenvalues of this coarse-grid correction operator C have a pole near a certain frequency index $\bar{j}$ whenever the product of the wave number k and the mesh size h satisfies $kh \leq 1$, thereby amplifying the associated error component. To alleviate this issue, a shifted wave number $\tilde{k}$, derived from dispersion correction, was introduced on the coarse grid in [7] to reduce the phase error and stabilize the coarse-grid correction. Furthermore, in [3] it was also shown that using such a modified wave number $\tilde{k}$ on the coarse grid to minimize numerical dispersion is essential for constructing efficient multigrid solvers. Here, we adopt a similar strategy; however, instead of using the tailored $\tilde{k}$ from [7, 3], we treat the modified wave number $\tilde{k}$, along with the damping parameters ω_i, as free parameters, and our goal is to determine the best values of $\tilde{k}$ and ω_i, i.e. values that yield the most efficient two-grid algorithm. We do this by numerically solving the min–max problem

$$\min_{\omega_i\in\mathbb{C},\tilde{k}\in\mathbb{R}} \max_j \left|\lambda_j\,(T)\right|, \quad T = S^{\nu_2}_{\omega_1,\ldots,\omega_s}\left(I - P\left(A_H(\tilde{k})\right)^{-1} RA(k)\right) S^{\nu_1}_{\omega_1,\ldots,\omega_s}, \tag{14}$$

where $A_H(\tilde{k})$ indicates that the dispersion correction has been incorporated by introducing the undetermined shifted wave number $\tilde{k}$ on the coarse grid. We note that in higher-dimensional cases, the numerical optimization of the associated min-max problem (14) remains standard, and the optimization procedure itself does not become fundamentally more complex. However, the derivation of the two-grid operator is technically more involved in higher dimensions. In particular, using a single shifted wave number on coarser grids is generally insufficient to provide an accurate correction of the numerical dispersion. Achieving improved dispersion in higher-dimensional settings typically requires more sophisticated discretizations or specialized stencils; see, for example, [2]. Extending the present approach to address these challenges will be the subject of future work.

We have now, both for the cavity and free space problems, the convergence factors $\rho(k, p, p_1, p_2)$ (see Eqs. (5)-(8)) for the Schwarz methods, as well as the two-grid operator T (see Eq. (11)) for the two-grid algorithm. In the next section, we will present a comprehensive numerical comparison of the convergence behaviors of these two iterative methods for cavity and free space problems.

4 Numerical Comparison of Schwarz and Multigrid

To evaluate and compare the performance of the Schwarz domain decomposition and multigrid methods, we examine the convergence behavior of both algorithms with respect to the original wave number k. For the two-grid method, two-step and four-step damped Jacobi smoothers with different numbers of smoothing steps ($\nu = \nu_1 + \nu_2$) are used. Here we assume that the number of pre- and post-smoothing steps are identical $\nu_1 = \nu_2$, and the fine and coarse grids Ω^h, Ω^H are chosen as $N = 31$, $h = \frac{1}{N+1} = \frac{1}{32}$, $n = \frac{N-1}{2} = 15, H = \frac{1}{n+1} = 2h = \frac{1}{16}$. Additionally, since our goal is to ensure convergence over a wide range of wave numbers–particularly those that may occur within a full multigrid cycle–we select a specific sequence of wave numbers by placing k^2 exactly between two Dirichlet eigenvalues[1], namely, for the given N, h,

$$k := k_l = \begin{cases} \sqrt{\frac{2}{h^2}\left(\sin^2\frac{(j-1)\pi h}{2} + \sin^2\frac{j\pi h}{2}\right)}, l = j, j = 1, \dots, N, \\ k_N + \sqrt{\frac{2}{h^2}\left(\sin^2\frac{(j-1)\pi h}{2} + \sin^2\frac{j\pi h}{2}\right)}, l = N + j, j = 1, \dots, N. \end{cases} \tag{15}$$

For the Schwarz methods we consider a symmetric two-subdomain decomposition of $\Omega := (0, 1)$ with $\Omega_1 = (0, \beta) := (0, \frac{1}{2} + \frac{L}{2})$, $\Omega_2 = (\alpha, 1) := (\frac{1}{2} - \frac{L}{2}, 1)$, where the overlap is $L = \beta - \alpha = 0.002$, and convergence is examined on a finer grid of wave numbers $k \in (0, 100]$.

It is worth noting that, for the OSM, we can determine the optimal transmission parameters by enforcing the numerators of $\rho_{\text{Opt}}^{\text{Cavity}}$ and $\rho_{\text{Opt}}^{\text{Free}}$ (see Eq. (6) and Eq. (8)) to vanish. This yields

$$p_{1,*}^{\text{Cavity}} = -\frac{k}{\tan k(\beta - 1)}, \quad p_{2,*}^{\text{Cavity}} = \frac{k}{\tan k\alpha}, \quad p_{1,*}^{\text{Free}} = p_{2,*}^{\text{Free}} = ik. \tag{16}$$

By using these optimal parameters, the OSM can achieve convergence in two iterations, effectively acting as a direct solver on the whole domain. This also implies that faster convergence is not possible.

However, these optimal choices can be realized in practice only in the 1D case, since in this case the parameters $p_{1,*}$ and $p_{2,*}$ are merely scalar values for a prescribed wavenumber k. In contrast, in higher dimensions, directly forcing the convergence factor to vanish results in optimal transmission parameters that correspond to non-local operators, making them impractical to implement. The best one can do in higher dimensions is to get an approximation of these optimal parameters [9, 11]. In order to faithfully reproduce the scenario in which approximate techniques are used in higher dimensions to approximate the optimal operators for computational feasibility, we do not use the optimal parameters (16) directly here; instead, we use a slight perturbation of them to represent their approximations, namely (note that for the symmetric decomposition in this example, the optimal $p_{1,*}^{\text{Cavity}}, p_{2,*}^{\text{Cavity}}$ have the

[1] This prevents the potential singularity induced by the Dirichlet boundary condition.

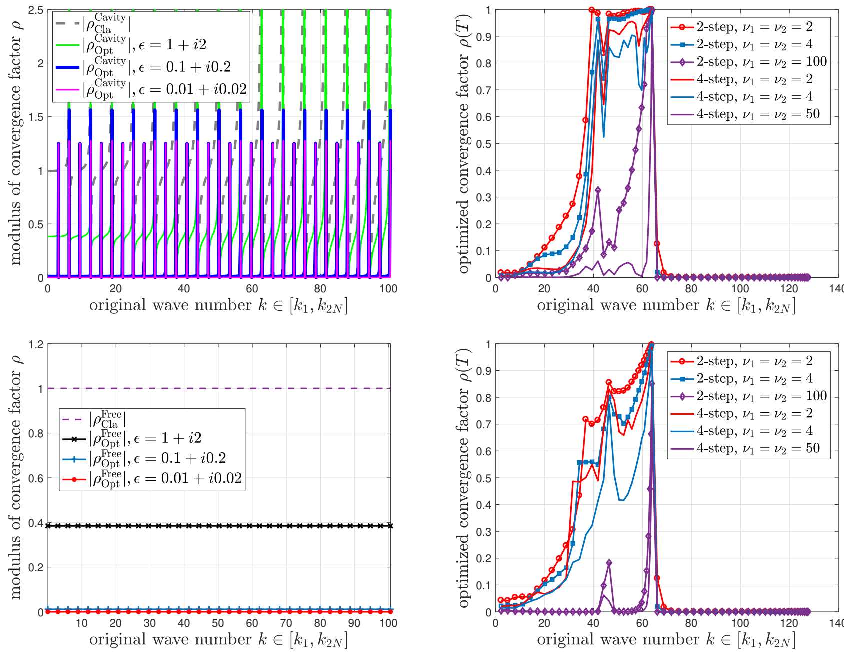

Fig. 1 Convergence factors as functions of the wave number k. Top left: Classical and optimized Schwarz methods with approximated optimal parameters (see Eq. (17)) for the cavity. Top right: Two-grid methods for the cavity. Bottom left: Classical and optimized Schwarz methods with approximated optimal parameters (see Eq. (17)) for the free space problem. Bottom right: Two-grid methods for the free space problem.

same values $\frac{k}{\tan k\alpha}$)

$$p^{\text{Cavity}}_{1,\text{app}} = p^{\text{Cavity}}_{2,\text{app}} = \frac{k}{\tan k\alpha}(1+\epsilon), \quad p^{\text{Free}}_{1,\text{app}} = p^{\text{Free}}_{2,\text{app}} = ik(1+\epsilon), \quad \epsilon \in \mathbb{C}. \tag{17}$$

To study how the Schwarz and two-grid methods contract for the cavity problem, we show in the first row of Fig. 1 the convergence factors as functions of the wave number k. From the numerical results shown in Fig. 1 on the top left, we see that for the cavity problem, the classical Schwarz method exhibits rapid divergence for many wave numbers k. The OSM with slightly perturbed optimal transmission conditions also shows difficulties to converge, even a very small perturbation ($\epsilon = 0.01 + i0.02$) of the optimal parameters causes convergence problems for certain values of k. Moreover, these convergence issues get rapidly worse as the perturbation increases. These observations indicate that in the cavity case, even a relatively accurate approximation of the optimal parameters can result in severe convergence degradation, demonstrating that the optimal transmission condition is highly sensitive to perturbations. An intuitive explanation for the severe oscillatory behavior observed in the convergence factor is that, the fully reflecting outer boundary traps wave energy inside the domain, leading to repeated reflections and the formation of cavity resonances at certain wave numbers. When these resonant modes interact with the Schwarz transmission conditions, the error is repeatedly re-injected into the interfaces rather than transported out of the domain, which can cause strong amplification and rapid divergence of the iteration. From the perspective of the convergence factor (6), this behavior is associated with near singularities arising from zeros (i.e., resonance frequencies) of the denominator. Although the exact cavity resonance frequencies are given by $k_n = n\pi$, for which the convergence factor can be shown to be identically equal to 1, the interaction between the transmission conditions and the fully reflecting boundary shifts these resonances to nearby wave numbers $\tilde{k}_n = n\pi + \delta_n$ with $\delta_n \ll 1$. These shifted resonances lead to the pronounced oscillations of the convergence factor observed in the numerical results. The precise locations of these $\tilde{k}_n$ are determined by a transcendental equation (i.e., zeros of the denominator of the convergence factor) and are not pursued further here.

The two-grid method shows similar convergence difficulties for the cavity problem, as seen in Fig. 1 on the top right, where the convergence factor remains close to 1 for wave numbers k between approximately $\hat{k} = \sqrt{2}/h$ and k_N. While additional smoothing steps sightly reduce the convergence factor, the improvement near k_N remains very limited. Although at the preset stage we do not have a definitive explanation for the convergence difficulties of the two-grid method in this wavenumber range, preliminary numerical experiments indicate that some eigenvalues of the Jacobi smoother, associated with high-frequency error components, are close to one and approach unity as the wavenumber nears k_N. This suggests that the observed deterioration is closely related to the reduced smoothing effectiveness of the Jacobi relaxation. A rigorous theoretical analysis of this behavior is left for future work.

In the second row of Fig. 1 we present the corresponding results for the free space problem, i.e., those with impedance outer boundary conditions. We see on the bottom left that although the classical Schwarz method still fails to converge, the OSM with approximated optimal parameters (17) shows robust and fast convergence for all wave numbers. Even when the perturbation increases (we have used the same perturbations, $\epsilon = 0.01 + i0.02$, $\epsilon = 0.1 + i0.2$ and $\epsilon = 1 + i2$, as in the cavity case), the OSM still converges very well, with the convergence factor uniformly less than 0.4. This indicates that for the free space problem, the OSM can achieve fast convergence even with a relatively rough approximation of the optimal parameters, and that the transparent transmission condition is robust to perturbations. In sharp contrast to the OSM, the two-grid method shows no substantial improvement in convergence compared to the cavity case, as illustrated in Fig. 1 on the bottom right. There still remain certain wave numbers k (particularly those around k_N) for which the two-grid method struggles to converge.

Finally, we remark that we have also tested several other standard smoothers (e.g., Kaczmarz iteration and GMRES) and observed comparable results. Therefore, for the sake of brevity, we focus our presentation on the results from the Jacobi smoother introduced earlier. Furthermore, in addition to the theoretically optimized convergence factors shown in Fig. 1, we also measured the actual numerical convergence factors of the Schwarz and multigrid methods. Some representative results are reported in

Table 1 Numerical convergence factors for Schwarz and multigrid methods

k \ Alg.	OSM (cavity) $\epsilon = 1 + i2$	OSM (free space) $\epsilon = 1 + i2$	Two-grid (cavity) 2-step, $\nu_1 = \nu_2 = 4$	Two-grid (free space) 2-step, $\nu_1 = \nu_2 = 4$
2.3	0.6201	0.6194	0.0078	0.0277
18.72	0.9401	0.6198	0.0844	0.0938
18.76	1.1201 (div.)	0.6157	0.0843	0.0903
60	0.4715	0.6200	0.9944 (slow)	0.8676 (slow)
62.4	0.9255	0.6193	0.9922 (slow)	0.9423 (slow)
62.6	1.3099 (div.)	0.6179	0.9914 (slow)	0.9492 (slow)
72.2	0.9092	0.6187	1.1405e-05	1.1323e-05
72.3	1.1600 (div.)	0.6193	1.0365e-05	1.0283e-05

Table 1, from which we observe that the convergence of the OSM depends strongly on the outer boundary condition, whereas that of the two-grid method does not. In particular, OSM diverges rapidly at certain wave numbers for the cavity problem but converges stably for the free space problem. The two-grid method, by contrast, exhibits consistent convergence behavior for both cavity and free space problems.

We thus see a clear difference in how outer boundary conditions affect the convergence of Schwarz and two-grid methods. For the Schwarz methods, convergence is much better for the free space problem than for the cavity problem, whereas for the two-grid method both cavity and free space problems remain equally hard to be solved.

5 Conclusions

We studied numerically the similarities and differences when using domain decomposition and multigrid methods to solve 1D Helmholtz problems. We observed that both methods fail to be effective for the 1D Helmholtz cavity problem, i.e. with Dirichlet outer BCs. For the free space problem however, with impedance outer BCs, optimized Schwarz methods can achieve fast convergence, while multigrid still struggles, as for the cavity problem.

While it was shown in [11] for higher dimensional Helmholtz problems why optimized Schwarz methods work much better for free space problems than for cavity (and wave guide) problems, it is currently not understood which free space problems are equally hard for multigrid methods like cavity problems. Explaining this and finding a remedy is our current focus of research.

References

1. Cocquet, P.H., Gander, M.J.: How large a shift is needed in the shifted Helmholtz preconditioner for its effective inversion by multigrid? SIAM J. Sci. Comput. **39**(2), A438–A478 (2017)

2. Cocquet, P.H., Gander, M.J., Xiang, X.: A finite difference method with optimized dispersion correction for the Helmholtz equation. In: International Conference on Domain Decomposition Methods, pp. 205–213. Springer (2017)
3. Cocquet, P.H., Gander, M.J., Xiang, X.: Dispersion correction for Helmholtz in 1D with piecewise constant wavenumber. In: International Conference on Domain Decomposition Methods, pp. 359–366. Springer (2018)
4. Dolean, V., Gander, M.J., Kyriakis, A.: Closed form optimized transmission conditions for complex diffusion with many subdomains. SIAM J. Sci. Comput. **45**(2), A829–A848 (2023)
5. Engquist, B., Ying, L.: Sweeping preconditioner for the Helmholtz equation: Moving perfectly matched layers. Multiscale Model. Sim. **9**(2), 686–710 (2011)
6. Erlangga, Y.A., Oosterlee, C.W., Vuik, C.: A novel multigrid based preconditioner for heterogeneous Helmholtz problems. SIAM J. Sci. Comput. **27**(4), 1471–1492 (2006)
7. Ernst, O.G., Gander, M.J.: Multigrid methods for Helmholtz problems: A convergent scheme in 1D using standard components. In: I.G. Graham, U. Langer, J.M. Melenk, M. Sini (eds.) Direct and Inverse Problems in Wave Propagation and Applications, pp. 135–186. De Gruyter (2013)
8. Gander, M.J., Graham, I.G., Spence, E.A.: Applying GMRES to the Helmholtz equation with shifted Laplacian preconditioning: what is the largest shift for which wavenumber-independent convergence is guaranteed? Numer. Math. **131**(3), 567–614 (2015)
9. Gander, M.J., Magoules, F., Nataf, F.: Optimized Schwarz methods without overlap for the Helmholtz equation. SIAM J. Sci. Comput. **24**(1), 38–60 (2002)
10. Gander, M.J., Zhang, H.: A class of iterative solvers for the Helmholtz equation: Factorizations, sweeping preconditioners, source transfer, single layer potentials, polarized traces, and optimized Schwarz methods. SIAM Rev. **61**(1), 3–76 (2019)
11. Gander, M.J., Zhang, H.: Schwarz methods by domain truncation. Acta Numer. **31**, 1–134 (2022)
12. Stolk, C.C.: A rapidly converging domain decomposition method for the Helmholtz equation. J. Comput. Phys. **241**, 240–252 (2013)
13. Stolk, C.C., Ahmed, M., Bhowmik, S.K.: A multigrid method for the Helmholtz equation with optimized coarse grid corrections. SIAM J. Sci. Comput. **36**(6), A2819–A2841 (2014)